



A Parametric Study on Improved Reduced Beam Section Connections with Post-tensioning to Enhance Seismic Resilience

R. Khandan, A. Sivandipour, E. Noroozinejad Farsangi*

Faculty of Civil and Surveying Engineering, Graduate University of Advanced Technology, Kerman, Iran

PAPER INFO

Paper history:

Received 28 April 2023

Received in revised form 10 June 2023

Accepted 09 July 2023

Keywords:

Post-tensioned Connections

Self-centering Connections

Reduced Section Beam Connections

Seismic Resilience

Finite Element Method

ABSTRACT

This study presents novel research on the seismic behavior of self-centering reduced beam section (RBS) connections in steel structures. Unlike traditional moment steel frames that concentrate non-elastic deformations in energy dissipation devices, the innovative self-centering RBS connections utilize post-tensioning techniques to restore the structure to its pre-earthquake condition. By significantly reducing residual deformations, these connections offer a promising alternative for improving seismic resilience. To validate the effectiveness of the post-tensioned (PT) and RBS connections, advanced nonlinear numerical modeling using the Finite Element Method (FEM) in ABAQUS software is employed. This approach allows for a comprehensive investigation, comparing the numerical results with laboratory data. Furthermore, the study goes beyond existing research by incorporating additional high-strength cables into the RBS connections. This novel configuration aims to assess the impact of post-tensioned cables on seismic behavior, adding a new dimension to the understanding of these connections. Through a rigorous parametric study, the research uncovers crucial insights into the seismic performance of the self-centering RBS connections. Notably, the study reveals the significant influence of the initial post-tensioning force on various aspects, including stiffness, maximum moment capacity, and gap-opening behavior of PT connections. The findings demonstrate the potential of increasing the initial post-tensioning force to enhance the energy dissipation capacity and overall performance of the PT connections. Overall, this study presents pioneering research that advances the understanding of self-centering RBS connections and their potential application in steel structures. By emphasizing the novel aspects of the research, it contributes to the body of knowledge in the field and provides valuable insights for improving the seismic resilience of structures.

doi: 10.5829/ije.2023.36.10a.11

1. INTRODUCTION

The rupture of the connection zone in steel structures' design is preferred to happen as the last step of the structure's failure after beams and columns' failure. Following the inappropriate behaviour of welded moment connections in the Northridge earthquake, there have been various details for moment connections in order to achieve a ductile response under seismic loading conditions. The goal of these connection details is to prevent weld rupture and to provide non-elastic deflections in beams and in an area out of the connection zone. Reduced Beam Section (RBS) is one of these

connection types. Weakening a part of the beam at a certain distance from the connection acts as a kind of safety switch that prevents connection problems. The performance of common systems resistant to lateral loads is dependent on the non-elastic behaviour of main structural elements. Hence these systems are inherently incapable of limiting the destruction or the residual drift. The new structures should provide desired behaviour in limiting the destruction and the incapacitated time. The post-tensioned connections have been suggested as a replacement to welded moment connections. This connection consists of high-strength steel cables that are laid along the beam's web, crossing the middle of column

* Corresponding Author Email: noroozinejad@kgut.ac.ir
(E. Noroozinejad Farsangi)

and face the column's web. The steel cables press the beam to the column resulting in sufficient moment resistance and returning force to bring the connection back to its initial position. Under the seismic loading, the connection opens, and a distance (crack) appears between the beam tensile wing and column. In this condition, the angles yield and play the role of energy dissipator. When the moment goes back to zero, the crack is closed, and the connection goes back to its initial condition, a process by which the residual deflections in beam and column is eliminated, and since the energy dissipation devices can easily be replaced, the cost of replacing these devices in post-tensioned connections will be less compared to the buckled beams in conventional moment frames [1-3]. This new type of steel connection was introduced by several researchers [4, 5]. The laboratory sample was utilized to acquire the cyclic response of the connection under investigation. In recent decades, there has been a growing interest in self-centering structures that can effectively return to their original positions. Previous research has explored various post-tensioned (PT) beam-column connections, considering different energy dissipative mechanisms. Previous studies utilizing ANSYS have demonstrated the reliability of employing monotonic analysis to assess the force-drift response of PT connections. These findings are further corroborated in the present paper through verification studies conducted with ABAQUS.

In contrast to previous models, which were limited in scope, comprehensive models were developed in this study to capture out-of-plane movement and beam local buckling behavior in PT connections. Although the viability of incorporating PT elements in steel frames has been confirmed in previous studies, current seismic design guidelines do not encompass regulations specifically addressing this application. Therefore, further research is necessary to thoroughly examine the seismic performance of PT connections and facilitate their widespread implementation in steel buildings. Finite-element (FE) analysis proves to be a valuable approach in investigating the seismic behavior of steel PT connections. FE models are cost-effective and allow for in-depth explorations of structural behavior, offering detailed insights into component behavior that may not be easily observable in experiments.

This paper also proposed the utilization of a reduced beam section to ensure the formation of a stable plastic hinge, effectively acting as a safety mechanism to mitigate connection issues. Additionally, it recommends incorporating additional reinforcement detailing in the contact region to delay yielding and buckling in the beam. In this study, the cyclic response of PT connections was evaluated by comparing it with experimental results conducted by Ricles et al. [6]. The assessment encompassed stiffness, moment capacity, energy dissipation, gap opening, local behavior, as well as stress

and strain distributions. Furthermore, parametric studies through simulations were conducted to explore the influence of initial post-tension forces on the cyclic response of PT connections.

Li et al. [7] presented post-tensioned connections with top and bottom angles. In this connection, the angles screwed to the beams flange play the energy dissipator. A Finite Element Method (FEM) was built of this connection, and they studied the effects of the details presented on the behaviour of the internal connection. To verify the model, 5 samples of the cruciform beam-to-column connection were tested. Furthermore, the time history analysis of six-storey steel frame with a post-tensioned connection was done. Then the results were compared to conventional welded connections, eventually depicting less residual displacement for frames with post-tensioned connections.

Fang et al. [8] studied the effects of factors such as dimension, the characteristics of top and bottom angles, the post-tensioning force amount in steel cables, and the presence of beam flange stiffening plates on the seismic response of beam-to-column connections. The results showed the flexural capacity and the energy dissipation levels are increased by using thicker angles. Also, it has shown that post-tensioned steel connections are a good replacement for conventional weld connections.

In order to study the behaviour of angles in bolted beam/column connections, Garlock et al. [9] tested 7 samples of these connections. In which, the effects of angle dimensions on connection's stiffness, strength and energy dissipation levels were defined. The goal of this study was to define the appropriate angle for post-tensioned connections. Ultimately the suggested angles had a good thickness, dimension, and material. Gerami [10] has investigated the steel moment frames using novel post-tensioned connections. Hosseinnejad et al. [11] investigated the use of smart materials (e.g., SMA) in post-tensioned connections.

Vasdravellis et al. [12] presented a new post-tensioned connection in which there were hourglass-shaped joints used beside the high-strength cables, that was responsible for energy dissipation. The connection was successful in eliminating residual deflection and avoiding damage to the main beams up to 6% drift. By iterating the tests, it was proven that the energy dissipation devices were easily replaced. Maghsoudi and Askari [13] have investigated the post-tensioned I-beams strengthened with CFRP.

Doostdar et al. [14] investigated post-tensioned external bars' effectiveness in strengthening reinforced concrete beams. ANSYS software and experiments confirm increased flexural capacity, decreased ductility. Higher impact observed with lower internal tension reinforcement percentages.

Moradi and Alam [15], presented a study on optimizing the lateral load-displacement of steel

connections in which they used RMS to predict and optimize the lateral response of beam-column connections with PT connection and top and bottom angles. The characteristics of lateral response that was studied in this paper include initial stiffness, load capacity, and the final displacement of PT connections. Based on FEM simulation, six parameters were considered as input variables in this study, namely, the post-tensioned force of the cable, beam depth, width and thickness of beam wing, span, and the height of the column. The goal of the optimization study is to maximize the initial stiffness, load capacity and ultimate drift of PT connections, and or minimize the amount of steel in the beam section which will result in reducing the final cost of structures. In the results, it's shown the more the depth of the beam and the higher the post-tensioned force in cables, the sooner the failure happens.

Some other researchers [2, 16-18] have been using open source platforms like OpenSees to investigate the damage index and seismic performance of building structures.

Sarvestani, [19] spent their time studying self-centering moment frames under near and far field earthquakes. In such a manner that the structural performance and seismic response of steel frames with self-centering moment frames with three various energy dissipation devices; namely top and bottom angles, friction devices of lower wing of the beam, and nut and bolt devices of the web; was studied. Then they were compared from the construction cost, energy dissipation and beam and column section dimensions.

Huang et al. [20] spent researching the initial stiffness of self-centering systems and its use in self-centering moment frame. The results of the tests on self-centering systems often showed a less initial stiffness to the predicted theoretical stiffness. Since the initial stiffness could have a special importance for controlled-deflection moment frames, in this study, they studied the definition of initial stiffness and the reasons for the difference between theoretical and experimental stiffness for some self-centering connection that were tested beforehand. Resulting in some suggestions to increase stiffness in these connections by reviewing the effective factors.

In another research, steel moment frames were exposed to 30 narrow band motions in various levels of earth motion intensity under spectrum acceleration in the first mode of vibration $S_a(T1)$, in order to conduct incremental dynamic analysis. The results are used to calculate the reliability of steel frame structures by using risk curves for residual displacements peak. It's been observed that the peak residual displacements that go past the 0.5% threshold are perceptible by residents and, based on recent studies can result in human discomfort. This is why using PTCs in steel frames is suggested to improve the reliability of the structure. The results showed the annual rate of surpassing the peak residual

storey drift is reduced by using PTC. Hence the reliability of steel frames with PTC is higher compared to normal moment frames [21].

Sofias and Pachoumis [22] tested two RBS connection models under cyclic loading and compared the results of lab model to the analytic model. All the characteristics of these two models, such as steel type, model's geometry, and beam/column dimensions were the same and the only difference was in the geometry of the RBS cut [22-25]. The geometry properties of the RBS are in Table 1.

Based on the results, both samples show similar failure, stiffness, and load-bearing capacity. Despite the different shapes of the RBS cut, the plastic zone was formed the same in both samples.

Bavandi et al. [24], with analyzing dispersion index focused on introducing an efficiency index for post-tensioned steel moment connections, with carrying out time history analysis and parametric studies on 3 models of steel buildings with post-tensioned connection (with various numbers of storeys) chose a model to evaluate and determining the efficiency index; then, a comparison and optimization was performed amongst the seven dispersion indexes that were introduced in the paper. Studies show that the efficiency index of PT connection, which is determined based on the change coefficient index, helps improve the speed and accuracy of the analyses.

In light of the deterioration of infrastructure and the increasing demand to reinforce structures to meet stringent design requirements, there has been a significant focus on the repair and strengthening of structures worldwide. Furthermore, seismic improvement of structures, particularly in regions prone to earthquakes, carries utmost importance. This study aims to explore the rehabilitation and strengthening of steel structures using reduced beam section (RBS) connections supplemented with post-tensioned cables integrated into the beams of the structure. Regrettably, no previous investigations have addressed the rehabilitation of steel structures through the incorporation of high-strength cables.

The primary objective of this paper is to comprehensively examine and evaluate the energy dissipation capacity, ductility, residual displacement, and seismic resilience of structures when employing these cables within steel frameworks. Through a thorough investigation, this study aims to shed light on the

TABLE 1. Geometric properties of RBS beam for RBS1 and RBS2 [22]

Specimen	(a) (mm)	(b) (mm)	(c) (mm)
RBS1 HEA180/60/75/25	108	128	45
RBS2 HEA180/45/75/20	81	128	36

potential benefits and performance implications of utilizing post-tensioned cables as a means of strengthening and rehabilitating steel structures.

2. MODELLING VERIFICATION

Since the topic is post-tensioned steel connections with reduced beam section, we have built a numerical model of one of the steel moment connections with top and bottom angles, and also a laboratory specimen of a beam connection with a reduced section in ABAQUS software. The results and characteristics from Ricles et al. [6] have been used to define the characteristics of the created post-tensioned numerical model and verification of the numerical model procedure. Hence we first introduced the laboratory specimen.

Ricles et al. [6] studied a few laboratories specimen under cyclic displacement loading. Figure 1 shows a schematic of these connections, between two beams and a column. In order to start the numerical model and verification of the results, the results from specimen pc4 that was post-tensioned by 4 steel cables on each side of the beam with an initial restricting force of 88.74 kN.

2. 1. Configuring the Model According to Figure 2, the model under study includes members with below sections:

- 1- Column: the column section is W14×311 profile, and the loading applied to the connection is applied by a hydraulic jack to the free end of the column and at 3658mm away from the joint connection at the base of the column.
- 2- Beam: the beam section is W24×163, and 28830.5mm long.
- 3- Top and bottom angles: for this application, an equal wings angle of 203mm and 15.9mm thickness is used.
- 4- To strengthen the beam wings, we have used sheets with 254×57×12.7mm dimensions.

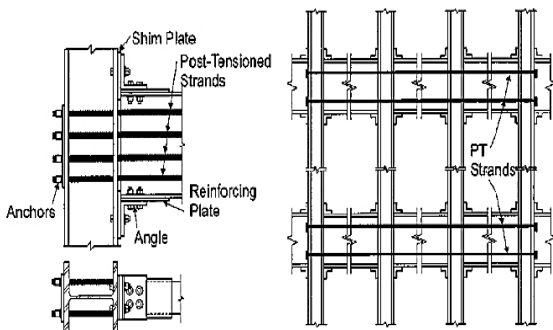


Figure 1. A- steel frame with post-tensioned connection with top and bottom angles B- the details of external connection of post-tensioned beam to column with steel cables [6]

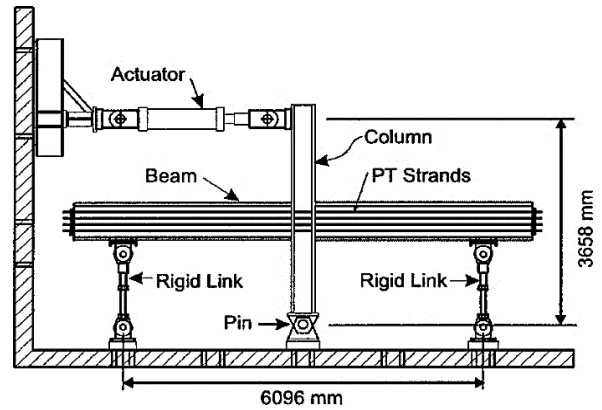


Figure 2. Schematic figure of lab model used in Ricles et al. [6]

- 5- Post-tensioned cables: section area of each cable is 140mm² and passes through a hole of 25mm made in the column’s wings.
- 6- To connect the top and bottom angles to column wings one bolt is used, and to the beam wings a 25.4 mm bolt is used.

The schematic depiction of the laboratory model used in Ricles et al. [6] research is given in Figure 2.

3. MATERIAL PROPERTIES

The yielding and ultimate stresses of the steel used in various configuring components are listed in Table 2.

The finite-element simulations in this study utilized the material properties reported in the reference experimental studies conducted by Ricles et al. [6]. A bilinear elasto-plastic stress-strain relationship was adopted for steel in all components, except for the bolts. High-strength bolts were modeled using a trilinear stress-strain relationship. The material models employed are illustrated in Figure 3.

TABLE 2. Properties of steel used in various parts of the lab specimen [6]

Piece	Yielding stress (MPa)	Plastic strain	Ultimate stress (Mpa)	Plastic strain
Post-tensioned cables	1305	0.00656	1864	0.0627
Stiffener plates	843	0.00421	895	0.0302
Shim plates	843	0.00421	895	0.0302
Angles	263	0.00131	465	0.0518
Beam web	266	0.00133	450	0.0933
Beam wing	230	0.00115	421	0.0967
Bolt	660	0.00330	830	0.074

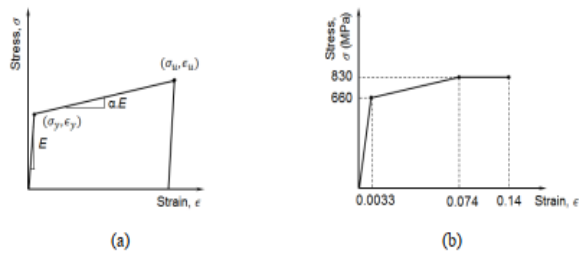


Figure 3. Idealized material behavior used in the finite element analysis: (a) bilinear kinematic hardening; (b) trilinear stress-strain steel model for bolts

In the material modeling, a strain hardening value of 0.05 was assigned for steel in post-tensioned (PT) strands, while a value of 0.02 was selected for steel in angles. For other components, a strain hardening ratio of 0.01 was assumed. Notably, a strain hardening ratio of 0.02 was chosen for angles to achieve improved predictions of the cyclic response after yielding occurred. Furthermore, a strain hardening ratio of 0.05 was considered for PT strands, based on a bilinear stress-strain relationship with a Young's modulus of 199 GPa, yield stress of 1,305 MPa, ultimate stress of 1,864 MPa, and an ultimate strain of 6%, as reported in the study by Ricles et al. [6]. The modulus of elasticity and Poisson's ratio for steel in other components were set at 200 GPa and 0.3, respectively.

4. BOUNDARY CONDITIONS AND LOADING

The support conditions for the beam were implemented in accordance with Figure 4. Specifically, roller support conditions were applied at a distance of 2,830.5 mm from the beam's length, resulting in a vertical displacement of zero. Additionally, the nodes located at the bottom of the column's centerline were constrained to have zero displacement, representing pin support conditions.

To subject the structure to loading, displacement was applied to the column flange. The loading protocol consisted of symmetric cyclic story drifts with amplitudes ranging from 0.1% to 3.5%. These story drifts were defined as the displacement applied to the column flange divided by 3,658 mm, following the approach by Ricles et al. [6].

Prior to conducting the analyses, preloads were applied to the bolts and post-tensioned (PT) bars. Subsequently, multiple load steps were defined to impose displacement drift cycles on the column. Nonlinear static analyses were performed to investigate the cyclic behavior of PT beam-column connections. The analyses accounted for large-deformation effects, incorporating geometric nonlinearity, material nonlinearity, and contact, which are recognized as contributing factors to

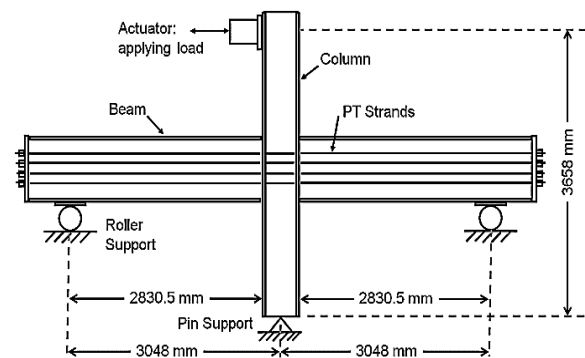


Figure 4. Support conditions of the lab specimen and numerical model of Ricles et al. [6]

nonlinear behavior. Notably, the models did not incorporate any initial geometric imperfections, focusing on capturing the buckling behavior of the structural components.

The applied force was a displacement cyclic loading, and the number of cycles and displacement amounts associated with each cycle are defined based on the protocol in SAC-97 for steel structures. Figure 5 depicts the relevant cycle for loading.

Later in the paper, the analytic model that is exactly the same as the laboratory model is modelled by Abaqus software. All parts of the model, except the post-tensioned cable, are made by solid elements, and in the post-tensioned cables, wire elements are used.

As shown in Figure 6, the various parts of the model are situated in appropriate places, geometrically. 8 high strength steel cables (4 on each side of the beam web) are located along the web's height.

5. MESHING

It is a prerequisite to numerical analysis to go through the meshing, and the elements of the model are divided to smaller elements. The configuring elements for all parts

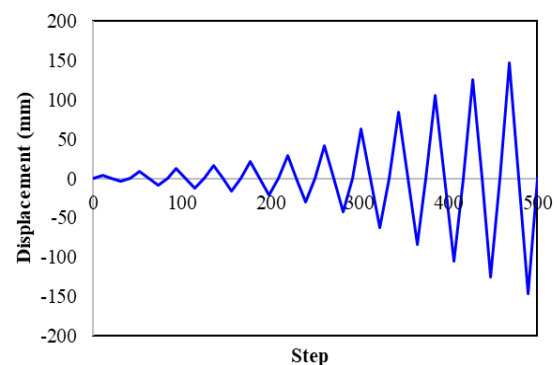


Figure 5. Loading protocol cycle used for this research [6]

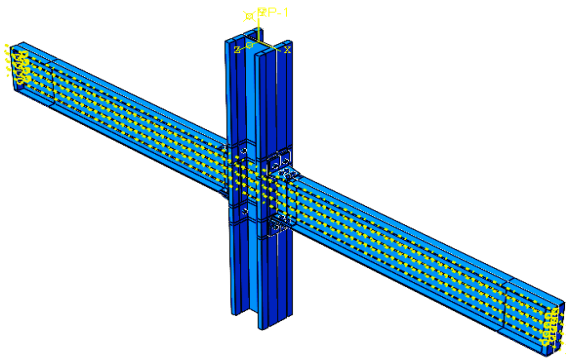


Figure 6. The assembly of consisting parts of the model, in their appropriate place, finalizing the model's geometry

are hexagonal 8-node elements (C3D8R) except the post-tensioned cables that were meshed using 2-node beam elements. The meshing is shown in Figure 7.

After appropriate meshing and getting geometric and appearance of the mesh in order, we can start solving the problem. To achieve the desired number of elements, first step we consider a main parameter that was the goal of the analysis (here it is the displacement of the point in column where the load applies), next step we increase the number of elements (resulting in reducing size of the elements) and repeat solving it in order to evaluate the effects of refining the mesh on the parameter at hand, to the point that there is an agreement between time and the number of the elements, in other words to the point where there is no particular change in the answer by the increase in the elements, or in fact the cost of the calculations outweighs the answers' changes. At this juncture, the model is deemed to be approaching convergence, thereby rendering superfluous the incorporation of additional constituents. Moreover, augmenting the number of elements would not significantly enhance the precision of the solution, but rather would solely result in the elongation of the solution time.

As shown in Figure 8, the size of the mesh and vertical axis in a calculation time curve and in another curve the displacement at load application point in 10 analysis, in the first curve first, the meshing is controlled against the calculation time. With refining the mesh size to 0.06 the calculation time shows no noticeable changes, but from 0.06 onward, the calculation time increases considerably. Another time the meshing is controlled from an accuracy point of view. As seen in the figure, the high displacement changes happen with mesh size changes at first, and curve's slope is high, as the mesh size reduces, the changes reduce too, and so does the curve's slope, to the point that it is almost zero slope.

6. CONTACT SURFACES

The model employed in this study encompassed various components, including columns, beams, angles,

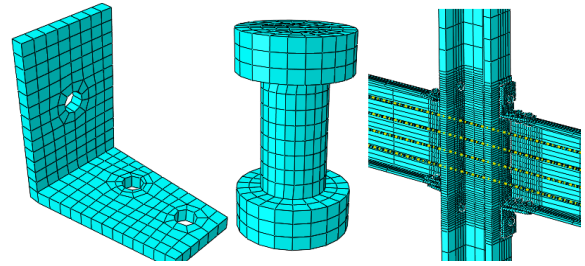


Figure 7. The model B meshing details (A) angles (B) Bolt (C) connection

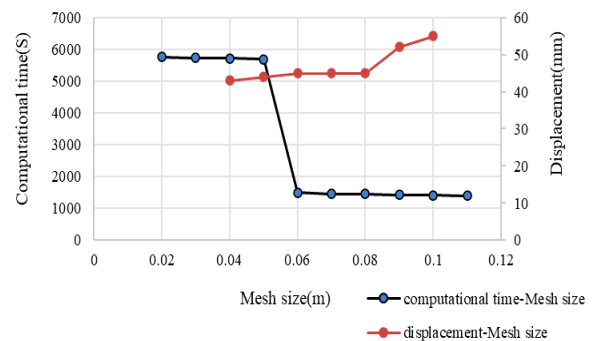


Figure 8. The mesh size curve to (A) analysis time (B) displacement

reinforcing plates, shim plates, bolts, steel post-tensioned (PT) strands, and anchorage plates located at the end of the beams. To ensure computational efficiency and manageable model sizes for finite element simulations of large-scale structural components, certain assumptions were made. Symmetry conditions were applied, resulting in the modeling of only half of the connection assembly. Furthermore, welding elements were not included in the models. However, the influence of welding was considered by imposing appropriate constraints on all degrees of freedom for relevant volumes, such as the beam flange and the beam reinforcing plate. This was accomplished through the application of Tie constraints to account for the welding effect.

To simulate the interaction between different components, contact elements were defined in both the vertical and tangential directions. Vertical interaction was modeled as hard contact, preventing penetration between contact element surfaces. A coefficient of friction of 0.4 was assigned to all contact elements. The following structural component interactions were considered: (a) angle leg and shim plate, (b) angle leg and beam flange, (c) beam web/flanges and shim plate, and (d) PT bars and holes in the column flanges.

In the ABAQUS software, specific options were utilized for the contact elements. The Gauss point detection option was employed to accurately determine the location of contact detection points. The penalty function was chosen as the contact algorithm.

Geometrical penetration or gap and offset were excluded in the analysis. Additionally, certain settings were adjusted to enhance convergence, particularly for the contact between PT bars and holes on the column flanges, which was identified as a potential source of non-convergence. Modifying the normal penalty stiffness factor for the contact element was one technique employed to avoid excessive contact stiffness that could lead to divergence. In Figure 9, the force-displacement hysteresis curve, which is derived from the numerical model in this study that, is compared to the results from Ricles et al. [6].

The results from the numerical model correspond to laboratory results. Also, by studying the two curves together, we can see that the maximum lateral force belongs to the laboratory model whereas the maximum force resulting from the numerical model is equal to 277.9 unit, which shows an error of 3%. Considering the low error between the maximum amounts of these graphs, for two numerical and analytic modes of analysis and also the similarity of behavior pattern and deformation of constituting elements of the connection in the numerical model made in ABAQUS software and laboratory sample used in Racheal et al. [6] study, we find out that the numerical model is made correctly. Now we can claim the derived results are reliable.

7. NUMERICAL MODELS

Two general models are considered in this study. The first group is denoted by RBS sign, in which the connection is the reduced section beam that are connected to the column by top and bottom angles. The second group is denoted by RBS+PT, which are similar to the first group in detail with the exception of having the post-tensioned cables along with the top and bottom angles.

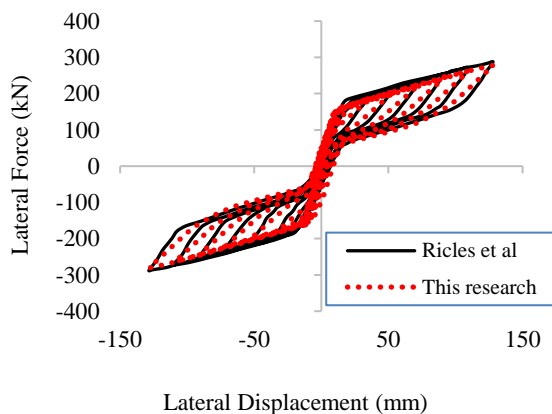


Figure 9. Comparing the results from numerical and laboratory model

7. 1. Steel Connections with Reduced Section (RBS)

In this model, the same details and beam and column dimensions of the verification model is used with the difference that the reduced section with geometric characteristics in Table 3 is used to move the plastic hinge from the critical zone, and also, the post-tensioned cables are deleted. In this connection, the beam and column are connected to each other by means of top and bottom angles.

7. 2. The Connection with Reduced Beam Accompanied by Steel Post-tensioned Cables

In this model same details of RBS model are used, the only difference is that there are 8 steel cables on both sides of the beam parallel to the beam's web, each one of which are post-tensioned by an initial force of 73.5kN. section area of each cable is 140mm² and crosses the 25mm holes that we created in the column's web. In this connection the beam and column are connected to each other by the means of top and bottom angles. (Figure 10) this model is identified by PT+RBS.

8. RESULTS AND DISCUSSION

The numerical RBS model results (RBS connections with angles and without steel cables) are listed in Table 4.

In this category of connections, the critical point of tension in the beam resides in the reduced section of the beam. In such way that the tension in beam web and near the reduced section of the beam or at the beam to column connection point. Based on RBS+PT model, the max tension in beam is 245MPa and located at the beam's web. The numerical RBS+PT model results (RBS connections with post-tensioned cables) are listed in Table 5.

The force-displacement hysteresis curve and push curve of RBS and RBS+PT models are shown in Figure 11.

TABLE 3. the geometric characteristics of reduced beam

Parameter	(a) (mm)	(b) (mm)	(c) (mm)
Value	134	391	30

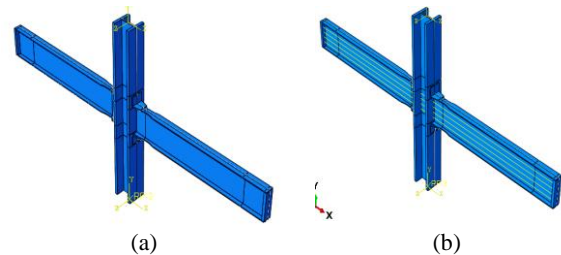


Figure 10. Connection with reduced beam section A- without PT cable, B- with PT cabl

TABLE 4. Results summary for RBS model analysis

Max plastic tension in angle	Max plastic tension in column	Max plastic tension in beam	Max tension in angle (MPa)	Max tension in column (MPa)	Max tension in Beam (MPa)
3.72E-3	0	4.078E-4	218	18.41	24.45

TABLE 5. Results summary for RBS+PT model analysis

Max plastic tension in angle	Max plastic tension in column	Max plastic tension in beam	Max tension in angle (MPa)	Max tension in column (MPa)	Max tension in Beam (MPa)
2.227E-2	1.774E-2	4.127E-2	186	107	245

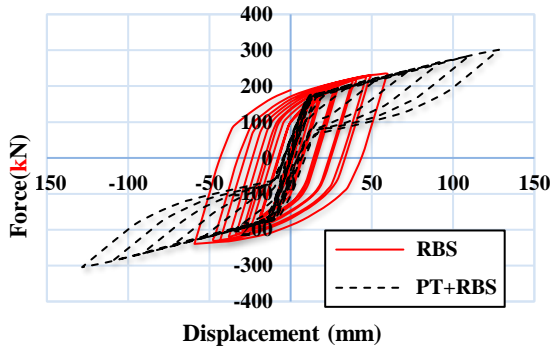


Figure 11. Comparison of RBS and RBS+PT hysteresis curves

Figure 12 shows the energy dissipation amounts along the analyzing time, resulting from plastic displacements which is summarized for RBS and RBS+PT models.

8. 1. Parametric Studies Parametric studies are used to study various parameters’ effects on the cyclic response of post-tensioned connections. The post-tensioning amount, the number of cables, the compound effect of force, and cable increase are the factors that are studied here.

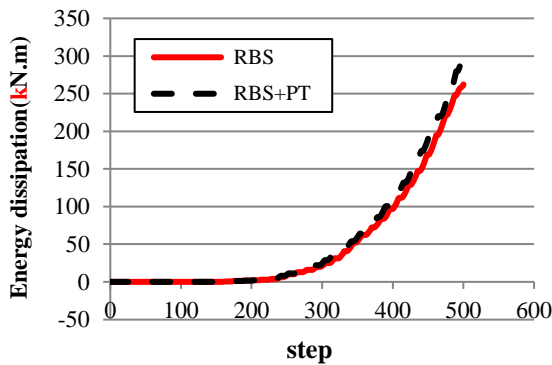


Figure 12. Energy dissipation of RBS and RBS+PT models due to plastic displacement

8. 2. Post-tension Force Effect The self-centering behavior of post-tensioned connections is highly dependent on the post-tensioning force in cables. RBS+PT sample was modeled to study the initial post tensioning force by considering three different levels of that. (RBS+PT0.45, RBS+PT0.5, RBS+PT0.6). In naming these models of these category, PT represents Post-tensioned, and the digits following that is the ratio of initial post-tensioning force to the cables ultimate tension (T_i/T_u). The ultimate force of post-tensioned cables is 261kN. The following introduces the types of models studied for these groups of connections.

8. 3. RBS+PT0.35 Model In this model the 8 cables are post-tensioned with a force equal to 91.87kN in each one of them (25% increase compared to RBS+PT model). the model is under cyclic loading. The force-displacement hysteresis curve compared to that of RBS+PT model is presented in Figure 13.

8. 4. RBS+PT0.45 Model In this model, the 8 cables are post-tensioned with force equal to 117.45kN in each one of them (60% increase compared to RBS+PT model). The model is under cyclic loading. The force-displacement hysteresis curve compared to that of RBS+PT model is presented in Figure 14.

8. 5. RBS+PT0.55 Model In this model, the 8 cables are post-tensioned with a force equal to 143.55kN

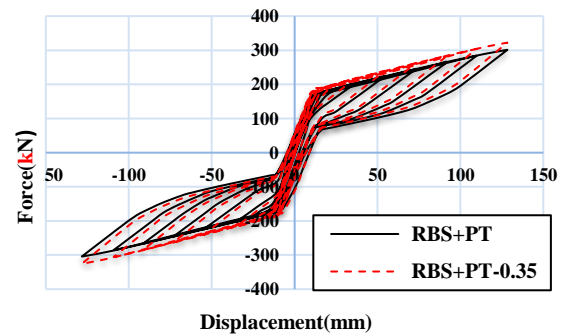


Figure 13. RBS+PT0.35 hysteresis curve compared to RBS+PT

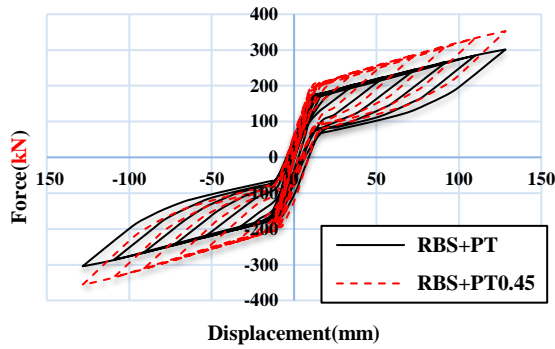


Figure 14. RBS+PT0.45 hysteresis curve compared to RBS+PT

in each one of them (95% increase compared to RBS+PT model). The model is under cyclic loading. The force-displacement hysteresis curve compared to that of RBS+PT model is presented in Figure 15.

The results show that the initial post-tensioning force will affect the stiffness and maximum flexural capacity of the post-tensioned connection.

All models and their responses are listed in Table 6. In this table, θ_r is the relative rotation angle between beam and the column. Other parameters in Table 6, T_i , F_{max} , M_{max} , Δ_{max} , K_i , K_P , and E_d respectively, show the initial post-tensioning force, maximum force, maximum moment, maximum displacement, initial stiffness, and energy dissipation. T_u is the ultimate force in each cable which here is considered to be 261kN. In this part also, the distribution of tensions and stains caused by the main connection elements is presented.

According to Table 6, the unloading happens sooner for connection with less initial post-tensioning (T_i), which is resulted in a bigger gap between beam and column. When the post-tensioning force is increased to 143.5 from 73.5 (almost a 95% increase), the maximum gap angle is reduced 7.32 percent. Also, the connection with higher T_i shows a 26.65% increase in flexural capacity (moment resistance) and a 26.95% increase in initial stiffness. It's worth noting, with increasing the T_i ,

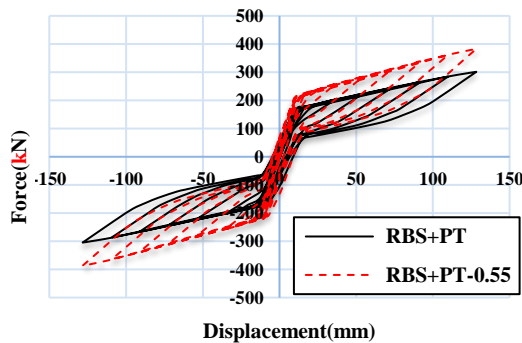


Figure 15. RBS+PT0.55 hysteresis curve compared to RBS+PT

TABLE 6. Responses under cyclic loading

Model	Ti/Tu	Ti (kN)	Mmax (kN.m)	θ_r (rad)	Ki (kN/m)	Ed (kN.m)
RBS+PT(0.28)	0.28	73.5	469	0.028	13302	290
RBS+PT0.35	0.35	91.8	503	0.027	14232	311
RBS+PT0.45	0.45	117.4	550	0.026	15556	469
RBS+PT0.55	0.55	143.5	597	0.025	16893	576
12CA-RBS+PT0.42	0.28	110.2	634	0.025	13302	666

the energy dissipation of RBS+PT connections is increased by almost 99% as the loading capacity of the PT sections is increasing.

Furthermore, the yielding spread and plasticizing the beams in connection with higher T_i is more intense. The beams in RBS+PT0.55 that has the highest post-tensioning force, and show a 75% bigger plastic strain (PEEQ) .

The simultaneous increase in the number of cables and the initial tensioning force. The cables are the main elements of PT connections, as the shear and moment are transferred from beam to column by means of the cables. Before the gap between the beam and column shows up, the behavior of these connections is under the effect of initial post-tensioning force, whereas the cables stiffness will be the most effective parameter in these connection's behavior. In this part, we keep the length and section area of the cables constant and change the number of those instead. In this way the cables' stiffness is proportionate to their number. In order to increase energy dissipation and improving the system's behavior, we studied the compound effect of increasing the number of cables and their post-tensioning force in the connection, 12CA=RBS+PT0.42 model with 12 post-tensioned cables, with details similar to RBS+PT model, and with post-tensioning force equal to 110.25kN (1.5 times of RBS+PT model's PT force) is modeled.

The force-displacement hysteresis curve of this connection is shown in Figure 16, based on these outcomes, with the increase in the number of cables, there

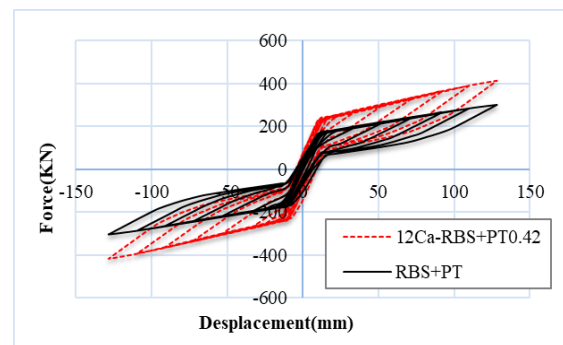


Figure 16. 12Ca-RBS+PT0.42 hysteresis model compared to RBS+PT

is an increase in flexural capacity as well as ductility. The connection with more cables, shows a more self-centering and restoring behavior.

9. SUMMARY AND CONCLUSION

While previous finite element (FE) studies have addressed certain types of post-tensioned (PT) connections, the modeling techniques required for different connections with distinct energy dissipative mechanisms may vary. Moreover, a comprehensive investigation focusing on the FE modeling of steel PT connections with top and seat angles and reduced beam connections (RBS) has not been previously presented. This study aims to address this gap by developing three-dimensional FE models to simulate the cyclic behavior of interior steel PT reduced beam-column connections with top and seat angles. The primary objective is to demonstrate the development of more detailed FE models using advanced features of the Abaqus software, showcasing the capabilities of numerical models in capturing the complex behavior of structural components. Notable features in Abaqus are utilized, such as the utilization of automated pretension elements and providing detailed explanations on modeling steps and options to mitigate convergence issues. Solid elements are employed to model connections to ensure comprehensive representation of local events. The analysis incorporates pretensioned bolts, material and geometric nonlinearity, and contact elements to simulate the behavior of steel PT connections.

This investigation encompasses a parametric analysis of three crucial factors influencing the cyclic behavior of PT connections: the number of post-tensioned cables, the magnitude of the initial post-tensioning force, and the incorporation of a beam web stiffener plate. PT steel connections offer an alternative to conventional rigid connections, overcoming associated limitations. The distinctive characteristic of this connection is the cyclic opening and closing of the gap between the beam and column intersection, facilitated by relative displacement and the restoring force of the cable. The top and bottom angles act as energy dissipators, ensuring effective energy dissipation. The study's findings can be summarized as follows:

- The proposed configuration demonstrates significant innovation, leading to improved seismic performance of the connection.
- Numerical analysis results exhibit strong agreement with laboratory findings, validating the reliability and accuracy of the models.
- All PT models exhibit minimal residual displacements, with cyclic behavior being influenced by factors such as PT cable yielding, local beam buckling, and angle rupture.

- Increasing the post-tensioning force in PT cables by 95% yields a 26.95% increase in stiffness, a 26.65% enhancement in flexural capacity, and an almost 99% escalation in energy dissipation, as indicated by the conducted parametric study.

10. REFERENCES

1. Horton, T.A., Hajirasouliha, I., Davison, B. and Ozdemir, Z., "Accurate prediction of cyclic hysteresis behaviour of rbs connections using deep learning neural networks", *Engineering Structures*, Vol. 247, (2021), 113156. doi: 10.1016/j.engstruct.2021.113156.
2. Guan, X., Burton, H. and Moradi, S., "Seismic performance of a self-centering steel moment frame building: From component-level modeling to economic loss assessment", *Journal of Constructional Steel Research*, Vol. 150, (2018), 129-140. doi: 10.1016/j.jcsr.2018.07.026.
3. Qian, K., Lan, X., Li, Z., Li, Y. and Fu, F., "Progressive collapse resistance of two-storey seismic configured steel sub-frames using welded connections", *Journal of Constructional Steel Research*, Vol. 170, (2020), 106117. doi: 10.1016/j.jcsr.2020.106117.
4. Hu, S., Wang, W., Alam, M.S. and Ke, K., "Life-cycle benefits estimation of self-centering building structures", *Engineering Structures*, Vol. 284, (2023), 115982. doi: 10.1016/j.engstruct.2023.115982.
5. Fang, C., Wang, W., Qiu, C., Hu, S., MacRae, G.A. and Eatherton, M.R., "Seismic resilient steel structures: A review of research, practice, challenges and opportunities", *Journal of Constructional Steel Research*, Vol. 191, (2022), 107172. doi: 10.1016/j.jcsr.2022.107172.
6. Ricles, J.M., Sause, R., Garlock, M.M. and Zhao, C., "Posttensioned seismic-resistant connections for steel frames", *Journal of Structural Engineering*, Vol. 127, No. 2, (2001), 113-121. [https://doi.org/10.1061/\(ASCE\)0733-9445\(2001\)127:2\(113\)](https://doi.org/10.1061/(ASCE)0733-9445(2001)127:2(113))
7. Li, S., Zhao, T., Alam, M.S., Cheng, Z. and Wang, J.-q., "Probabilistic seismic vulnerability and loss assessment of a seismic resistance bridge system with post-tensioning precast segmental ultra-high performance concrete bridge columns", *Engineering Structures*, Vol. 225, (2020), 111321. doi: 10.1016/j.engstruct.2020.111321.
8. Fang, C., Qiu, C., Wang, W. and Alam, M.S., "Self-centering structures against earthquakes: A critical review", *Journal of Earthquake Engineering*, (2023), 1-36. doi: 10.1080/13632469.2023.2166163.
9. Garlock, M.E.M., "Design, analysis, and experimental behavior of seismic resistant post-tensioned steel moment resisting frames, Lehigh University, (2003).
10. Gerami, M., "Multi-stage performance upgrade of steel moment frames by post-tension connections", *International Journal of Engineering, Transactions B: Applications*, Vol. 34, No. 5, (2021), 1132-1144. doi: 10.5829/ije.2021.34.05b.07.
11. Hosseinnejad, H., Lotfollahi-Yaghin, M., Hosseinzadeh, Y. and Maleki, A., "Numerical investigation of response of the post-tensioned tapered steel beams with shape memory alloy tendons", *International Journal of Engineering, Transactions A: Basics*, Vol. 34, No. 4, (2021), 782-792. doi: 10.5829/ije.2021.34.04a.04
12. Vasdravellis, G., Karavasilis, T.L. and Uy, B., "Large-scale experimental validation of steel posttensioned connections with web hourglass pins", *Journal of Structural Engineering*, Vol.

- 139, No. 6, (2013), 1033-1042. doi: 10.1061/(ASCE)ST.1943-541X.0000696.
13. Maghsoudi, A. and Askari D, Y., "Ultimate unbonded tendon stress in CFRP strengthened post-tensioned indeterminate I-beams cast with HSCs", *International Journal of Engineering, Transactions C: Aspects*, Vol. 28, No. 3, (2015), 350-359. doi: 10.5829/idosi.ije.2015.28.03c.03.
 14. Doostdar, H., Nemati, M. and Naghi Pour, M., "Experimental study and modeling of reinforced concrete beams strengthened by post-tensioned external reinforcing bars", *International Journal of Engineering, Transactions A: Basics*, Vol. 23, No. 2, (2010), 127-144.
 15. Moradi, S. and Alam, M.S., "Lateral load-drift response and limit states of posttensioned steel beam-column connections: Parametric study", *Journal of Structural Engineering*, Vol. 143, No. 7, (2017), 04017044. doi: 10.1061/(ASCE)ST.1943-541X.0001772.
 16. Al Kajbaf, A., Fanaie, N. and Najarkolaie, K.F., "Numerical simulation of failure in steel posttensioned connections under cyclic loading", *Engineering Failure Analysis*, Vol. 91, (2018), 35-57. doi: 10.1016/j.engfailanal.2018.04.024.
 17. Mazzoni, S., McKenna, F., Scott, M.H. and Fenves, G.L., "The open system for earthquake engineering simulation (OpenSees) user command-language manual", *University of California, Berkeley: Pacific Earthquake Engineering Research Center*, Vol. 2006, (2006).
 18. Mazloom, M. and Fallah, N., "Seismic vulnerability assessment of existing RC moment frames using a new stiffness based damage index", *International Journal of Engineering, Transactions B: Applications*, Vol. 36, No. 5, (2023), 1000-1011. doi: 10.5829/ije.2023.36.05b.16.
 19. Sarvestani, H.A., "Structural evaluation of steel self-centering moment-resisting frames under far-field and near-field earthquakes", *Journal of Constructional Steel Research*, Vol. 151, (2018), 83-93. doi: 10.1016/j.jcsr.2018.09.013.
 20. Huang, X., Eatherton, M.R. and Zhou, Z., "Initial stiffness of self-centering systems and application to self-centering-beam moment-frames", *Engineering Structures*, Vol. 203, (2020), 109890. doi: 10.1016/j.engstruct.2019.109890.
 21. Bojorquez, E., Lopez-Barraza, A., Reyes-Salazar, A., Ruiz, S.E., Ruiz-García, J., Formisano, A., Lopez-Almansa, F., Carrillo, J. and Bojorquez, J., "Improving the structural reliability of steel frames using posttensioned connections", *Advances in Civil Engineering*, Vol. 2019, (2019). doi: 10.1155/2019/8912390.
 22. Sofias, C. and Pachoumis, D., "Assessment of reduced beam section (RBS) moment connections subjected to cyclic loading", *Journal of Constructional Steel Research*, Vol. 171, (2020), 106151. doi: 10.1016/j.jcsr.2020.106151.
 23. Shen, P.-W., Yang, P., Hong, J.-H., Yang, Y.-M. and Tuo, X.-Y., "Seismic performance of steel frame with a self-centering beam", *Journal of Constructional Steel Research*, Vol. 175, (2020), 106349. doi: 10.1016/j.jcsr.2020.106349.
 24. Bavandi, M., Moghadam, A.S., Mansoori, M.R. and Aziminejad, A., "Introducing a new seismic efficiency index of post-tensioned self-centering steel moment connections", in *Structures*, Elsevier, Vol. 33, (2021), 463-483.
 25. Horton, T.A., Hajirasouliha, I., Davison, B., Ozdemir, Z. and Abuzayed, I., "Development of more accurate cyclic hysteretic models to represent RBS connections", *Engineering Structures*, Vol. 245, (2021), 112899. doi: 10.1016/j.engstruct.2021.112899.

COPYRIGHTS

©2023 The author(s). This is an open access article distributed under the terms of the Creative Commons Attribution (CC BY 4.0), which permits unrestricted use, distribution, and reproduction in any medium, as long as the original authors and source are cited. No permission is required from the authors or the publishers.

**Persian Abstract****چکیده**

با توجه به استفاده گسترده از فولاد در ساختمان سازی و اهمیت زیاد اتصالات فولادی در این ساختمان‌ها، این پژوهش عملکرد لرزه‌ای اتصالات RBS بهبود یافته با سیستم مرکزگرا را برای سازه‌های فولادی مورد بررسی قرار می‌دهد. اتصالات پس‌کشیده مرکزگرا به عنوان جایگزینی برای اتصالات قاب خمشی فولادی مرسوم، با تمرکز تغییرشکل‌های غیرالاستیک در وسایل اتلاف انرژی و بازگرداندن سازه به حالت اولیه قبل از وقوع زلزله، دارای عملکرد مناسبی تحت بار زلزله می‌باشند و این رفتار خودمرکزیت اتصالات با کاهش تغییرشکل‌های پسماند، وجه تمایز اینگونه اتصالات پس‌کشیده با سایر اتصالات خمشی متداول می‌باشد. در این پژوهش، با استفاده از مدلسازی عددی در نرم افزار ABAQUS به روش اجزا محدود، به مدلسازی ترکیبی اتصالات پس‌کشیده PT و RBS و صحت‌سنجی نتایج آنها در مقایسه با نتایج آزمایشگاهی پرداخته شده است، سپس دو مدل RBS جزئیات یکسان مدلسازی گردیده و جهت بررسی اثر کابل‌های پس‌کشیده، یکی از مدل‌ها بوسیله ۸ عدد کابل پرمقاومت، پس‌کشیده شده است و نتایج دو مدل با یکدیگر مقایسه شده است. در ادامه با انجام مطالعات پارامتریک تأثیر سه پارامتر بر عملکرد لرزه‌ای این اتصالات مورد ارزیابی قرار گرفته است. پارامترهای مورد بررسی در این تحقیق شامل مقدار نیروی پس‌کشیدگی اولیه و افزایش تعداد کابل می‌باشند. نتایج به دست آمده نشان می‌دهند که اتصالات دارای کابل پس‌کشیده، شکل‌پذیری خوب، اتلاف انرژی قابل قبول و قابلیت برگشت‌پذیری مناسبی دارند.